

February 2007  
Vol. 21, No. 1  
www.i-LEOS.org



# IEEE LEOS

NEWS

THE SOCIETY FOR PHOTONICS

*Discrete Optics in Liquid  
Crystalline Lattices*

*Special 30th Anniversary Feature:  
Most Cited Article from IEEE  
Journal of Quantum Electronics*

*Chaotic  
Microcavity  
Lasers*

# University Research Highlights

## Chaotic microcavity lasers

H. Cao, W. Fang<sup>1</sup>, E. E. Narimanov<sup>2</sup>, V. A. Podolskiy,<sup>2,3</sup> and G. S. Solomon<sup>4</sup>

### Abstract

We reviewed our recent studies on chaotic microcavity lasers. Although most microcavities are designed to have regular shapes, boundary roughness, which is introduced unintentionally during the fabrication process, can throw the regular ray dynamics into chaos. Fortunately, the dynamical localization makes the perform-

ance of microcavity lasers robust with respect to the boundary roughness and corresponding ray chaos. In a chaotic microcavity, the lasing modes may be pulled away from the cavity boundary to avoid the reduction of lasing gain by surface recombination. Moreover, the carriers injected to the central region of a cavity can contribute to lasing. Despite counter-intuitive, a chaotic microcavity laser could produce directional output beams. Unfortunately the threshold of chaotic microcavity lasers is usually high. We demonstrated that the lasing threshold in a fully chaotic open microcavity can be minimized by tailoring its shape factor.

### Introduction

#### A. Why chaos is related to a microcavity laser

Microcavity lasers are expected to realize an extremely high efficiency and high speed by the volume effect and the spontaneous emission control. Over the past two decades, there have been rapid developments of microcavity lasers. To see how chaos is relevant to microcavity lasers, let us consider an example - microdisk laser [1]. In a dielectric disk of circular shape [Figs. 1(a) and (b)], optical rays form a series of whispering-gallery (WG) trajectories with conserved angle of incidence  $x$  and correspondingly, conserved angular momentum (in the unit of  $\hbar$ )  $m = (2\pi nR/\lambda_0) \sin\chi$  ( $R$  being the disk radius,  $n$ , the refractive index of the dielectric,  $\lambda_0$  the vacuum wavelength). Since the refractive escape is only possible for the trajectories with  $\chi$  below the critical angle  $\chi_c = \arcsin(1/n)$  the rays with  $\chi > \chi_c$  are trapped inside the dielectric microdisk by the total internal reflection. The cavity modes corresponding to these trajectories can therefore leave the resonator only via evanescent escape, thus they usually have extremely long lifetimes and low lasing threshold.

Unfortunately, any deviation from the perfectly circular disk due to, e.g. boundary roughness, would inevitably break this idealized picture. It destroys the rotational symmetry and can make the classical ray dynamic chaotic. As a ray trajectory propagates in such a disk, its angle of incidence  $\chi$  changes in a quasi-random manner, until it becomes less than  $\chi_c$  when the ray may refractively escape from the system [Figs. 1(c) and (d)]. Hence, from the view point of geometric optics, the boundary roughness

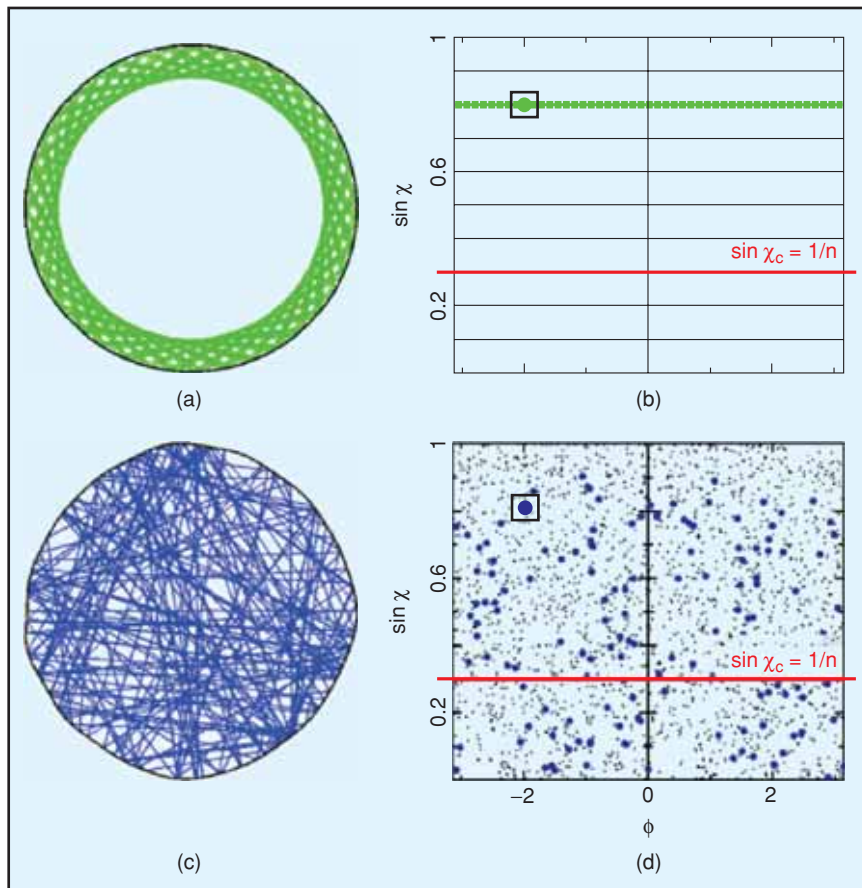


Figure 1: Ray trajectories inside a circular microdisk have whispering-gallery (WG) structure (a). The angular momentum of any given trajectory is conserved due to the symmetry of the microdisk boundary. This fact is clearly seen in the Poincaré surface of section (SOS) (b), consisting of a series of one-dimensional lines, each corresponding to an orbit with fixed angle of incidence  $\chi$ . The green dots correspond to the trajectory in (a), bold dot in the black square denotes the starting point. The trajectories with  $\chi > \chi_c = \arcsin(1/n)$ , where  $n$  is the refractive index of the cavity, are trapped by total internal refraction (red line corresponds to experimental value  $n = 3.25$ ). Introduction of roughness to the microcavity boundary destroys the stability of all WG orbits (c). Total ray chaos is illustrated through the system's SOS, shown on panel (d). The single trajectory now explores all available phase space, and may classically escape from the resonator when its  $\sin\chi$  is below  $1/n$ ; Blue dots show the trajectory in (c), which has the same initial conditions as in the trajectory in (a) [bold blue dot in the black square].

1. DEPARTMENT OF PHYSICS AND ASTRONOMY, NORTHWESTERN UNIVERSITY, EVANSTON, IL 60208
2. ELECTRICAL ENGINEERING DEPARTMENT, PRINCETON UNIVERSITY, PRINCETON, NJ 08544
3. PHYSICS DEPARTMENT, OREGON STATE UNIVERSITY, CORVALLIS, OR 97331
4. SOLID-STATE PHOTONICS LABORATORY, STANFORD UNIVERSITY, STANFORD, CA 94305; AND ATOMIC PHYSICS DIVISION, NIST, GAITHERSBURG, MD 20899-8423.

could significantly reduce the lifetime of light in a microdisk, and dramatically increase the lasing threshold. Despite the rapid advances in nanofabrication technologies, the boundary roughness for GaAs microdisks is still 10-20nm. Recent calculations show that the boundary roughness as small as 20nm could throw the regular ray dynamics in a microdisk into chaos [2]. The qual-

ity ( $Q$ ) factor for a GaAs microdisk of radius =  $5\mu\text{m}$  drops from  $10^{13}$  in the absence of boundary roughness to  $10^3$  in the presence of 20nm boundary roughness. This example illustrates that although most microcavities are designed to have regular shapes, chaos can be introduced unintentionally as a result of imperfection in nanofabrication, and it could have significant impact on the performance of microcavity lasers.

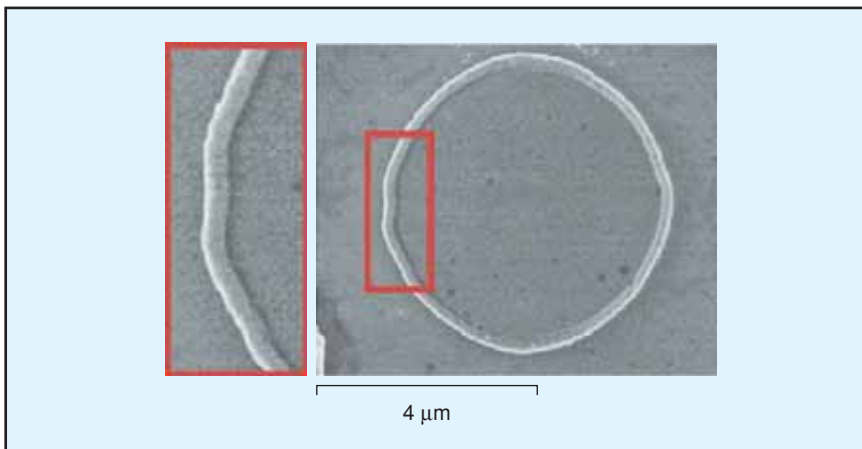


Figure 2: Top-view scanning electron micrograph of a GaAs microdisk. The disk has rough near-circular boundary with an average radius of approximately  $2.6\mu\text{m}$ .

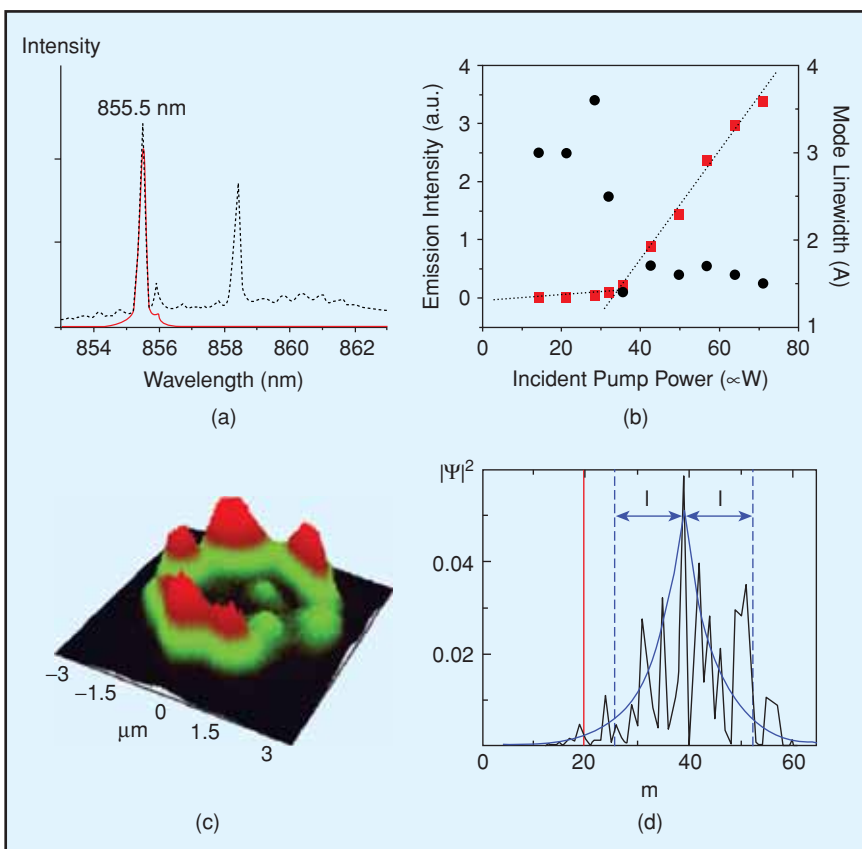


Figure 3: Spectrum of emission from the microdisk in Fig. 2 at the incident pump power of  $44\mu\text{W}$  (a) clearly shows multi-mode lasing (black dotted line). A bandpass filter of 1nm bandwidth selects a single lasing mode at 855.5nm (red line). The onset of lasing oscillation in this mode (b) is confirmed by the rapid increase of the emitted intensity as a function of the pump power (red squares) and simultaneous decrease of the linewidth (black circles) when pump reaches the threshold of  $35\mu\text{W}$ . The near-field optical image of this lasing mode is shown in (c). (d) is the calculated angular momentum distribution of this lasing mode, which serves as a clear evidence of the dynamical localization with localization length  $l = 12.4$ . The  $Q$ -factor of the mode is  $4.78 \times 10^3$ .

## B. How chaos can be utilized for microcavity laser

One problem for semiconductor microcavity lasers is nonradiative recombination of injected carriers via surface electronic states. As the cavities get smaller, the surface to volume ratio is increased. The resonant modes have more overlap with the cavity boundaries, facilitating the surface recombination. Let us again take the microdisk laser as an example. As the radius of a circular disk decreases, the whispering-gallery modes are pushed towards the disk boundary. The close proximity of the lasing mode to the cavity boundary where the optical gain is reduced by surface recombination leads to an increase of the lasing threshold.

To reduce the detrimental effect of surface recombination on a semiconductor microcavity laser, we utilize a chaotic microcavity to pull the lasing modes away from the boundary. The disk shape is deformed from circle so that the lasing modes are no longer WG modes. If the modes stay mostly in the interior of a microdisk, the reduction of lasing gain by surface recombination is minimized. A second advantage of pushing the lasing modes to the interior of a microdisk is to utilize the carriers there for lasing gain. In a circular microdisk, the carriers near the disk center do not contribute to lasing in the WG modes. Such carrier loss is more significant for the case of electrical pumping, because carriers are usually injected to the central region of a microdisk. The third advantage of a chaotic microcavity laser, which may seem counter-intuitive, is that it could produce directional output beams. Despite these advantages, the quality factor of a chaotic microcavity is usually low, leading to high lasing threshold. The question we intend to address is whether and how we can minimize the lasing threshold in a chaotic microcavity.

## Microdisk Laser with Rough Boundary

Figure 2 is the scanning electron micrograph (SEM) of a circular microdisk [3]. It is made of 200nm-thick GaAs layer with a thin InAs quantum well (QW) in the middle serving as

the gain medium. The disk radius is approximately  $2.6\mu\text{m}$ . The microdisks are fabricated by photolithography and two steps of wet etch. Each disk is supported by a 500nm-long AlGaAs pedestal. The magnified SEM in the left panel of Fig. 2 reveals the roughness at the disk boundary. Such degree of roughness is significantly larger than what can be achieved with the state-of-the-art nanofabrication. Nevertheless, we realized lasing in such a rough disk with decent threshold.

The lasing experiment is performed on individual disks which are optically pumped by a mode-locked Ti-sapphire laser at 790 nm. Figures 3(a)-(d) show the results of measurement on the microdisk in Fig. 2. As shown in Fig. 3(a), the emission spectrum features a broadband amplified spontaneous emission (ASE) and several distinct peaks that correspond to the cavity modes. Fig. 3(b) is a plot of the intensity and linewidth of one mode at  $\lambda=855.5\text{nm}$  as a function of the incident pump power. When the pump power exceeds a threshold, the emission intensity exhibits a sudden increase accompanied by a simultaneous decrease of the mode linewidth. This threshold behavior corresponds to the onset of lasing oscillation in this mode. Using a narrow bandpass filter, we took the near-field image of this lasing mode on the top surface of the disk shown in Fig. 3(c). The lasing mode is spatially localized near the boundary of the rough disk, similar to the WG mode in a perfectly circular disk.

However, the classical ray dynamics in a rough disk is very different from that in a perfectly circular disk [4]. We digitized the SEM in Fig. 2 to obtain the exact size and shape of the microdisk we measured, and found the ray dynamics in this disk is completely chaotic. Figure 1(c) shows a typical ray trajectory which spreads over the entire disk. Correspondingly in the angular momentum space, the ray undergoes a chaotic diffusion, as shown in Fig. 1(d). However, the measured lasing mode profile [Fig. 3(c)] does not resemble any chaotic ray trajectory. This dramatic difference is caused by interference effect which is neglected in ray optics. We solved the wave equation to find the resonant modes in the microdisk shown in Fig. 2. We identified the observed lasing modes with the calculated cavity modes of small decay rates. Those modes are located close to the disk boundary. Figure 3(d) shows the intensity distribution of one such mode in angular momentum space. Unlike a WG mode with constant angular momentum  $m$ , this mode contains many angular momentum components. However it is not uniformly distributed in  $m$ , but localized in a region above the critical value  $m_c = (2\pi nR/\lambda_0)\sin\chi_c$ . This localization results from the interference effect, namely, the interference of scattered light suppresses the chaotic diffusion of optical rays in angular momentum space. It is called dynamical localization [5-7]. When a mode is localized in the region  $m > m_c$ , the refractive escape rate is low. That is why we can get lasing with relatively low threshold.

### Microstadium Laser

We intentionally made chaotic microcavity lasers because of their advantages mentioned in the introduction section. This section is focused on the stadium-shaped microcavity. The classical ray dynamics in a stadium billiard is fully chaotic [8]. However, a dense set of unstable periodic orbits (UPOs) are embedded in the sea of chaotic orbits. Despite of their zero measure, UPOs manifest themselves in the eigenstates of the system via "scars", i.e., extra concen-

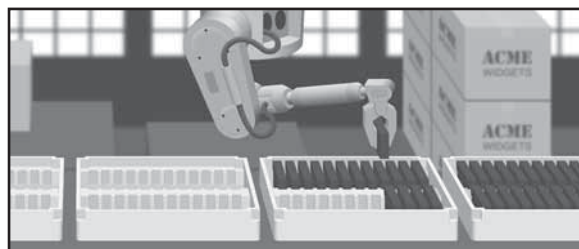
trations of eigenstate density near UPOs [9]. In the past few years, lasing was realized in both scar modes and chaotic modes of semiconductor stadiums with certain major-to-minor-axis ratio [10,11]. Highly directional output of laser emission was predicted [12] and confirmed in polymer stadiums [13]. Unfortunately, the lasing threshold in dielectric microstadiums is quite high. Our goal is to find out how to minimize the lasing threshold in such an open chaotic microcavity.

Contrary to common expectation, our numerical study revealed that modes of a dielectric microstadium could have long lifetime [14]. These special modes are typically scar modes corresponding to unstable periodic orbits with incident angles above the critical angle  $\chi_c$ . If a scar mode consists of several UPOs, the interference of partial waves propagating along the constituent orbits may minimize light leakage at certain major-to-minor-axis ratio [14]. This means the lasing threshold should be sensitive to the stadium shape, i.e., the major-to-minor-axis ratio.

To confirm this numerical result, we fabricated GaAs microstadium lasers [15]. The layer structure consists of 500nm AlGaAs and 200nm GaAs. In the middle of the GaAs layer there is a thin InAs QW. The lower refractive index of AlGaAs layer leads to the formation of a slab waveguide in the top GaAs layer. Stadium-shaped cylinders were fabricated by photolithography and wet chemical etch. The major-to-minor-axis ratio of the stadiums was varied over a wide range while the stadium area remains nearly constant. The deformation of a stadium is defined

## MATERIAL HANDLING TRAYS FOR PARTS PROCESSING

- **Clean room compatible**
- **Static dissipative certification**
- **Smooth surfaces**
- **Low mold costs for custom designs**
- **Rapid turnaround**
- **Low quantities available**



**TEMPO**  
PRECISION MOLDED FOAM

[www.tempo-foam.com](http://www.tempo-foam.com) 559-651-7711

as  $\epsilon \equiv a/r$ , where  $2a$  is the length of the straight segments connecting the two half circles of radius  $r$ .

In the lasing experiment, individual microstadiums were optically pumped by a mode-locked Ti-sapphire laser. Lasing was realized in most stadiums with  $\epsilon$  ranging from 0.4 to 2.2 and area  $\sim 70\mu\text{m}^2$ . Figure 4(a) shows the emission spectra of twelve stadiums slightly above their lasing thresholds so that we mainly see

their first lasing modes. As  $\epsilon$  increases, the first lasing mode jumps back and forth within the gain spectrum of InAs QW. It is not always located near the peak of gain spectrum ( $\lambda \sim 857\text{nm}$ ). At some deformation, e.g.  $\epsilon = 0.94, 1.9$ , the first lasing mode is far from the gain maximum. This phenomenon is not caused by lack of cavity modes near the maximum of gain spectrum. A few small and broad peaks in the emission spectrum between 847nm and

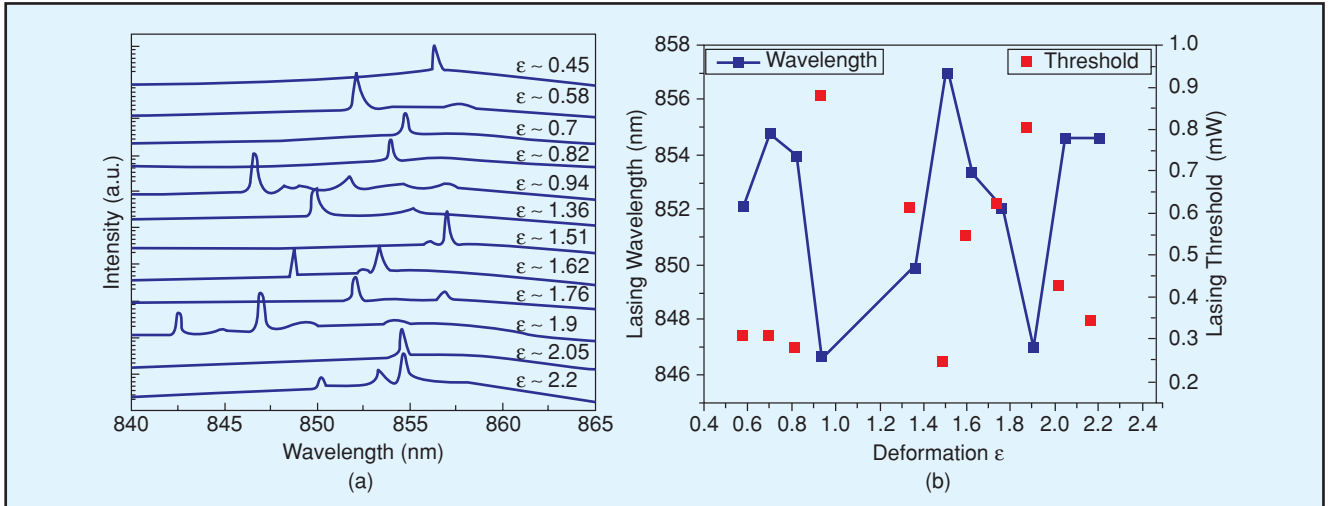


Figure 4: (a) Lasing spectra from twelve GaAs microstadiums with different deformations. (b) Wavelength and lasing threshold of the first lasing mode as a function of  $\epsilon$ .

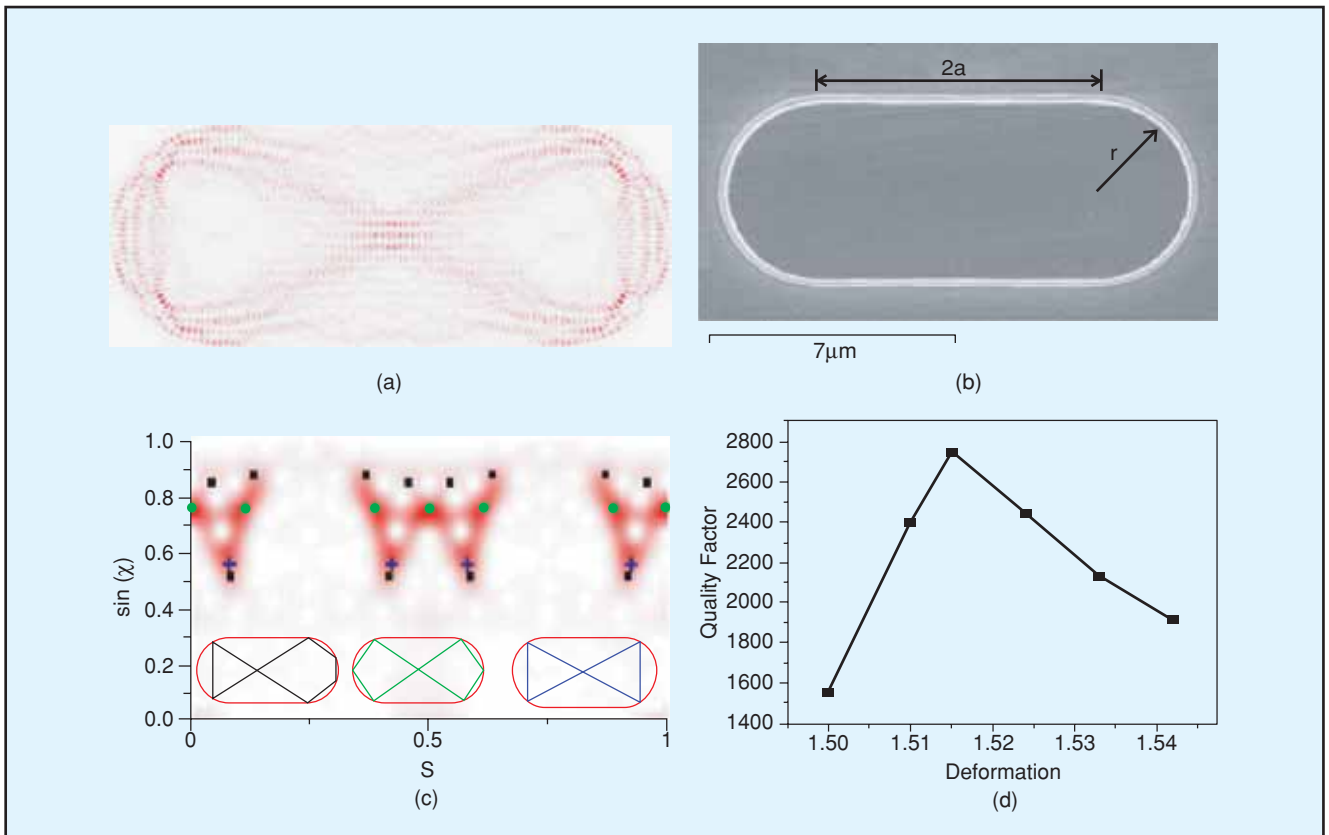


Figure 5: (a) Calculated intensity distribution of the first lasing mode in the GaAs microstadium of  $\epsilon = 1.51$ . The wavelength of the mode is 850.7nm. (b) Top-view SEM of the stadium, from which the exact size and shape of the stadium is extracted for calculation. (c) Husimi phase space projection of the mode in (a). The horizontal coordinate  $s$  represents the length along the stadium boundary from the rightmost point, normalized by the stadium perimeter. The squares, dots and crosses mark the positions of three different types of UPOs shown in the inset. (d) Calculated Q-factor of the mode in (a) as a function of  $\epsilon$ .

857nm represent the cavity modes. These modes experience higher gain than the lasing mode at  $\lambda \approx 847\text{nm}$ . The only reason they do not lase is their quality factors are low. This result indicates the lasing modes, especially the first one, must be high- $Q$  modes. However, when the lasing mode is away from the maximum of gain spectrum, the relatively low optical gain at the lasing frequency results in high lasing threshold. This is confirmed in Fig. 4(b), which shows the lasing threshold strongly depends on the spectral distance between the first lasing mode and the maximum of gain spectrum.

Figure 5(a) shows the calculated intensity distribution of the first lasing mode at  $\lambda = 850.7\text{nm}$  in the microstadium with  $\epsilon = 1.51$ . To find out the classical ray trajectories that this lasing mode corresponds to, we calculated the Husimi phase-space projection of this lasing mode from its electric field at the stadium boundary [Fig. 5(c)]. It reveals the lasing mode is a scar mode, and it consists mainly of three different types of UPOs plotted in the inset of Fig. 5(c). The constituent UPOs are above the critical line for total internal reflection, thus the lasing mode has small decay rate. We calculated the quality factor of this mode in passive stadium as the deformation  $\epsilon$  is varied around 1.51. As shown in Fig. 5(d), its  $Q$  value first increases then decreases as  $\epsilon$  increases, leading to a maximum at  $\epsilon = 1.515$ . Such variation of quality factor is attributed to interference of waves propagating along the constituent UPOs. The interference effect depends on the relative phase of waves traveling in different orbits. The phase delay along each orbit changes with the orbit length as  $\epsilon$  varies. At some particular deformation, constructive interference may minimize light leakage out of the cavity, thus maximizing the quality factor. Since the actual deformation  $\epsilon = 1.51$  is nearly identical (within 0.3%) to the optimum deformation ( $\epsilon = 1.515$ ), the mode is almost at the maximum of its quality factor. Furthermore, its frequency is close to the peak of gain spectrum. Thus the lasing threshold is minimized, as shown in Fig. 4(b).

## Conclusion

We reviewed our recent studies on chaotic microcavity lasers. Although most microcavities are designed to have regular shapes, boundary roughness, which is introduced unintentionally during the fabrication process, can throw the regular ray dynamics into chaos. Fortunately, the interference of scattered light can suppress the chaotic diffusion of rays and result in dynamical localization of the lasing modes. It makes the performance of microcavity lasers robust with respect to the boundary roughness and corresponding ray chaos.

Chaotic microcavity lasers have several advantages compared to the regular microcavity lasers. We demonstrated that lasing in a fully chaotic open microcavity can be optimized by tailoring its shape factor. Fine tuning of the cavity shape allows us not only to optimize light confinement inside the cavity but also extract the maximum gain by aligning the mode frequency to the peak of gain spectrum. The simultaneous realization of the lowest cavity loss and the highest optical gain minimizes the lasing threshold.

## Acknowledgments

We acknowledge Prof. Fritz Haake, Prof. Peter Braun and Dr. G.G. Carlo for stimulating discussions. This work is supported partly by NIST under the Grant No. 70NANB6H6162 and by NSF under

the MRSEC program (DMR-00706097) at the Materials Science Center of Northwestern University.

## References

- [1] S. L. McCall, A. F. J. Levi, R. E. Slusher, S. J. Pearton, and R. A. Logan, "Whispering-Gallery Mode Microdisk Lasers," *Appl. Phys. Lett.*, Vol. 60, pp. 289-291, 1992.
- [2] A. I. Rahachou and I. V. Zozoulenko, "Scattering matrix approach to the resonant states and  $Q$  values of microdisk lasing cavities," *Appl. Opt.*, Vol. 43, pp. 1761-1772, 2004.
- [3] V. A. Podolskiy, E. E. Narimanov, W. Fang, and H. Cao, "Chaotic microlasers based on dynamical localization. Proceedings of the National Academy of Sciences of the United States of America," Vol. 101, pp. 10498-10500, 2004.
- [4] W. Fang, and H. Cao, V. A. Podolskiy, and E. E. Narimanov, "Dynamical localization in microdisk lasers," *Optics Express*, Vol. 13, pp. 5641-5652, 2005.
- [5] K. M. Frahm and D. L. Shepelyansky, *Phys. Rev. Lett.*, Vol. 78, pp. 1440-1443, 1997.
- [6] L. Sirko, Sz. Bauch, Y. Hlushchuk, P. M. Koch, R. Blümel, M. Barth, U. Kuhl, and H.-J. Stöckmann, "Observation of dynamical localization in a rough microwave cavity," *Phys. Lett. A* Vol. 266, pp. 331-335, 2000.
- [7] O. A. Starykh, P. R. J. Jacquod, E. E. Narimanov, and A. D. Stone, "Signature of dynamical localization in the resonance width distribution of wave-chaotic dielectric cavities," *Phys. Rev. E*, Vol. 62, pp. 2078-2084, 2000.
- [8] M. C. Gutzwiller, *Chaos in Classical and Quantum Mechanics* (Springer, Berlin, 1990).
- [9] E. J. Heller, "Bound-State Eigenfunctions of Classically Chaotic Hamiltonian-Systems - Scars of Periodic-Orbits," *Phys. Rev. Lett.*, Vol. 53, pp. 1515-1518, 1984.
- [10] T. Harayama, T. Fukushima, P. Davis, P.O. Vaccaro, T. Miyasaka, T. Nishimura, and T. Aida, "Lasing on scar modes in fully chaotic microcavities," *Phys. Rev. E*, Vol. 67, 015207, 2003.
- [11] T. Harayama, P. Davis, and K.S. Ikeda, "Stable oscillations of a spatially chaotic wave function in a microstadium laser," *Phys. Rev. Lett.*, Vol. 90, 063901, 2003.
- [12] H. G. L. Schwefel, N. B. Rex, H. E. Tureci, R. K. Chang, A. D. Stone, T. Ben-Messaoud, and J. Zyss, "Dramatic shape sensitivity of directional emission patterns from similarly deformed cylindrical polymer lasers," *J. Opt. Soc. Am. B*, Vol. 21, pp. 923-934, 2004.
- [13] M. Lebental, J. S. Lauret, R. Hierle, and J. Zyss, "Highly directional stadium-shaped polymer microlasers," *Appl. Phys. Lett.*, Vol. 88, pp. 031108, 2006.
- [14] W. Fang, A. Yamilov, and H. Cao, "Analysis of high-quality modes in open chaotic microcavities," *Phys. Rev. A*, Vol. 72, 023815, 2005.
- [15] W. Fang, G. S. Solomon, and H. Cao, "Control lasing in fully chaotic open microcavities by tailoring the shape factor," arXiv:physics/0607223.